DECAY OF THE BARYON-RICH QUARK-GLUON PLASMA PRODUCED IN RELATIVISTIC HEAVY-ION COLLISIONS

By B. Kämpfer, H. W. Barz, L. Münchow

Zentralinstitut für Kernforschung Rossendorf*

and B. Lukács

Central Research Institute for Physics, Budapest**

(Received December 13, 1985)

The decay of a baryon-rich quark plasma is considered on three levels, i.e. a) hydrodynamic expansion with either sudden or delayed phase transition and viscosity; b) bubble creation and growth; and c) redistribution of quarks into hadrons. The calculations indicate that slow deflagration of bubbles may be a physical process leading to rehadronisation, while detonation and bulk transition seem to require both supercooling in plasma state and overheating of the hadronic matter. Some estimates relying on classical nucleation theory are presented. The redistribution model introduces statistical weights according to different numbers of possible final states. Large yields of kaons and lambdas are predicted.

PACS numbers: 14.80.Dq, 47.75.+f

1. Introduction

The existence of a deconfinement phase transition (at high density and/or temperature) is more or less generally accepted; the resulted deconfinement state is called quark-gluon plasma [1]. Such a state may be expected in heavy ion collisions [2], and experiments are being planned. Of course, the plasma state should be identified in measurements. One can expect that direct photons and leptons can be emitted during the whole lifetime of the plasma, while other particle yields and rapidity distributions are connected rather with the decay of the plasma.

The plasma, if produced in a relativistic heavy ion collision, recombines into hadrons during the hydrodynamic expansion. In the majority of papers dealing with hadronisation the central rapidity region (with small or zero baryon number) has been considered; for this case detailed calculations exist for the evolution [2] and the lattice calculations

* Address: Zentralinstitut für Kernforschung Rossendorf, DDR-8051, Dresden Pf. 19., GDR
** Address: Central Research Institute for Physics, H-1525 Bp. 114. Pf. 49. Budapest, Hungary.

for the equation of state are rapidly being improved [3–7]. However, other cases are important too; here we investigate the decay of a baryon-rich plasma, produced either in the fragmentation region of an ultrarelativistic collisions [8] or in a relativistic collision of large stopping power [9, 10]. We consider the global hydrodynamic expansion of plasma blobs either with sudden or with delayed phase transition; as approximation both spherical and plane flow geometries will be used. Our goal is to study the time scales of the existence and decay of the plasma, the extra entropy production due to non-equilibrium phase transitions, the expansion patterns and the possibility of the formation of a condensation front. As pointed out recently [7], relaxation phenomena, as e.g. the delayed phase transition or bulk viscosity, alter the space-time history of the plasma, thus affecting the plasma signatures too.

Here the rehadronisation process is considered on the bubble level, within the framework of the classical nucleation theory; thus, the previous analyses [4, 6] are extended to the baryon-rich plasma. The mentioned hadronising models rely on the assumption of an equilibrated hadronic state, which then can be simply described by an equation of state. Nevertheless even then one does not have a reliable equation of state at disposal. Therefore we are going to utilize a convenient parametrized form relying on a nucleon and a pion component. Combining this with the plasma equation of state a two phase model is obtained which is conform to the known lattice results for vanishing baryon number.

Since an assumption of final hadron equilibrium is rather strong and calculations based on the flux tube model [3, 4] indicate that it might be unrealistic for small systems created in heavy ion collisions and expanding freely, here we elaborate a model for the statistical redistribution of the quarks into hadrons, and compare it to the equilibrium model. The predicted hadron yields are discussed as tools of plasma identification.

In Sect. 2 we consider the hydrodynamic expansion of plasma blobs. Different types of bubble growth and physical processes across discontinuities are studied in Sect. 3. The statistical model for quark redistribution is presented in Sect. 4, finally the conclusions are given in Sect. 5.

2. *Hydrodynamic expansion of plasma blobs*

A dynamical phase transition is a complex process with strong interplay between phase transition kinetics and global dynamics. Here we consider the global dynamics of expanding plasma blobs, with some simplifications in the phase transition. Two different simplifying assumptions will be used, namely first a sudden transition, and then a delayed one with a linearized relaxation law. For technical reasons spherical and plane-symmetric flow geometries are used; the tackled problems are the time scales, expansion pattern, viscosity effects and the extra entropy production.

The hydrodynamic equations are the familiar balance equations

$$T^{ir}{}_{;r} = 0, \tag{2.1}$$

$$(nu^r)_{;r} = 0, \tag{2.2}$$

(where T^{ik} stands for the energy-momentum tensor, n is the baryon density, u^i is the four-velocity, while the semicolon denotes covariant derivative), solved in Lagrangian coordinates as described in Ref. [11].

The equation of state is approximated as follows. The quark-gluon plasma is described by the bag model

$$P_q = -B + \tfrac{37}{90}\pi^2 T^2 + \mu^2 T^2 + \frac{1}{2\pi^2}\mu^4,$$

$$n_q = \tfrac{2}{3}\mu\left(T^2 + \frac{1}{\pi^2}\mu^2\right), \tag{2.3}$$

$$e_q = 3p_q + 4B,$$

where p, T, μ and e are the pressure, temperature, chemical potential and energy density, respectively, and B stands for the bag constant, $B^{1/4} = 235$ MeV is accepted here. The hadronic matter is built up from two components; for the nucleon component a parabolic compression term + thermal Boltzmann term are used:

$$e_n = n\left(m_n + K\left(\frac{n}{n_0} - 1\right)^2 + \tfrac{3}{2}T\right), \tag{2.4}$$

where m_n is the nucleon mass, n_0 is the ground state density and $K = 280$ MeV, while for the pionic component, for convenience's sake, a massless equation of state is used:

$$e_\pi = \frac{\pi^2}{10}T^4. \tag{2.5}$$

The presented model possesses a critical exponent $\beta = 1/3$ (according to numerical experience) which fact allows to fit the density jump in phase coexistence by the one-third power law

$$n_q - n_{n+\pi} = A(T_c - T)^\beta, \tag{2.6}$$

with $A = 0.1338\ \text{MeV}^{-1/3}\ \text{fm}^{-3}$. This relation holds down to $T = 0.8\,T_c$, where

$$T_c = \left(\frac{90}{34\pi^2}B\right)^{1/4} \tag{2.7}$$

is the critical temperature.

Now we are going to discuss two particular approximations for the phase transition process:

Case a) *Sudden phase transition*

In this approximation the Maxwell construction is used to match the equations of state of different phases. This is physically satisfactory if the microscopic processes behind nucleation and bubble growth are fast enough compared to the characteristic time of hydrodynamic evolution. Since viscosity is neglected, the expansion is isentropic.

Let us consider first initial conditions appropriate for states which might be achieved in heavy ion collisions. For definiteness' sake $T = 70$ MeV, $n = 2.2\ \text{fm}^{-2}$ and $A = 400$

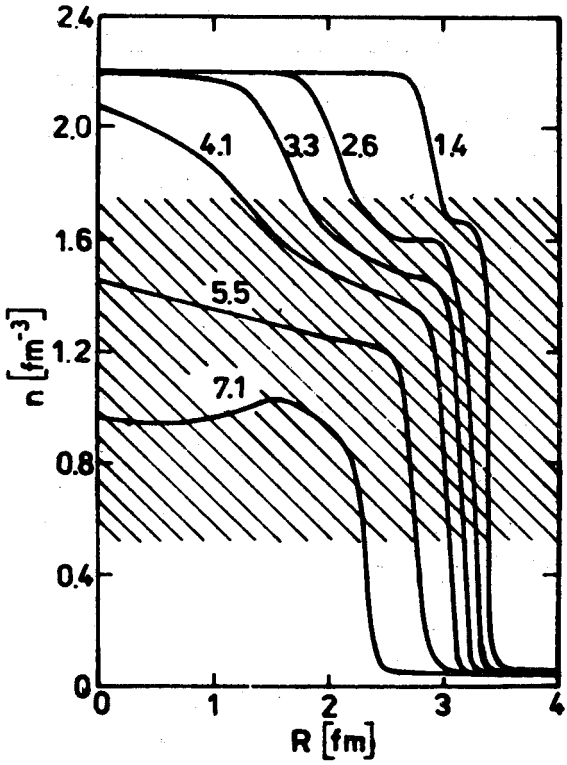

Fig. 1a

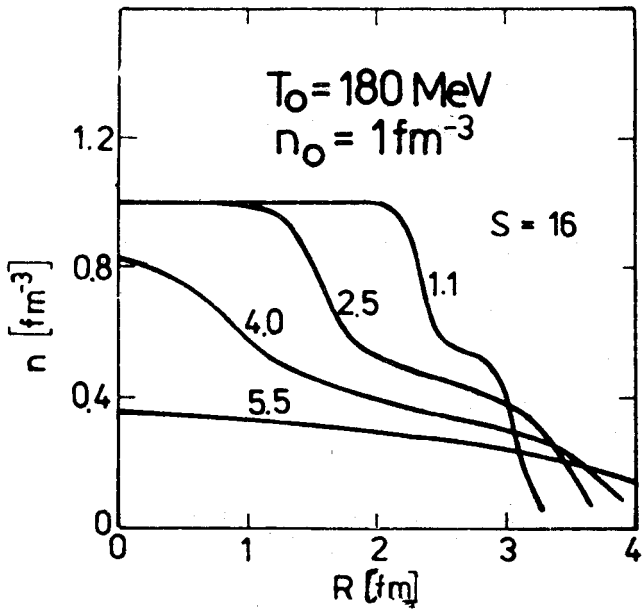

Fig. 1b

Fig. 1. Snapshots of density profiles during spherical hydrodynamical expansions. Time values meant in fm/c.a) Initial density $n = 2.2$ fm^{-3} and initial temperature $T = 70$ MeV (the hatched area indicates the coexistence region on the isentrope), b) initial density $n = 1$ fm^{-3}, initial temperature $T = 180$ MeV

are chosen as an example for extreme dense and cool plasmas. This set represents a state whence a deflagration without supercooling is possible (cf. Sect. 3). Fig. 1a displays the snapshots of density profiles in a spherical expansion. At the beginning of the expansion the density profiles are similar to a "double shock front". There is a front in which the plasma is cooling down isentropically to a state at the phase boundary or slightly inside the coexistence region. Because of the rapid change of the sound velocity (cf. Fig. 2a), there arises a plateau with states composed from more than 90% plasma. Behind the plateau there is a sharp front in which hadronic state is reached. According to our approximation, the cells are decoupled from the hydrodynamic evolution if their baryon density falls below a break-up density chosen as $n_{bu} = 0.05\,\mathrm{fm}^{-3}$ here.

The spatial structure can be visualized as a shrinking plasma blob surrounded by a thin hadronic shell whence hadrons are ejected into vacuum. (A similar picture was developed in Ref. [4] for $\mu = 0$.) The plasma lifetime is ca. 8 fm/c, the separating front moves with a velocity $v \sim 0.1\,c$ (thus comparable to the condensation front velocity in Sect. 3). Later a rarefaction wave appears.

Obviously the expansion pattern may depend on the assumed symmetry, therefore now we are going to compare the above spherical situation to a plane-symmetric one. Fig. 2a displays the density profiles for slab geometry with the same initial conditions as above, the initial length is that for uranium compressed to $n = 2.2\,\mathrm{fm}^{-3}$. The plane-symmetric expansion is similar to the spherical one, nevertheless with 1) a shorter plasma lifetime, due to the small size of the drop; 2) a stronger rarefaction wave; and 3) a stronger plateau in the density profiles due to the sudden decrease in the sound velocity.

Of course, the present example relies on our ignorance of transparency and sideward flow at $E_{beam}/A \sim 5$ GeV. Possibly more relevant initial conditions for the fragmentation region are $3\,n_0 < n < 5\,n_0$, and temperature close to deconfinement temperature. Thus for the second example we choose $n = 1\,\mathrm{fm}^{-3}$, $T = 180$ MeV and blobs of $N = 100$. The snapshots of these density profiles for spherical expansion are shown on Fig. 1b. No inward moving separating front appears, rather the blob expands. Typical paths on the phase diagram are given in Ref. [12].

Case b) *Delayed phase transition*

If the characteristic time of nucleation and bubble growth is not negligible compared to that of the expansion, some relaxation processes are to be taken into account. These non-equilibrium processes may be quite complicated; here we adopt the simplified model described in Refs [11–13]. We assume that thermal and mechanical equilibrium are much faster achieved than the chemical one. Neglecting surface effects one can write

$$W(n, T) = \alpha W_1 + (1-\alpha) W_2, \tag{2.8}$$

where W is the specific energy, the lower indices label the phases, W_i is given by Eqs (2.3)–(2.5), while α is the relative weight of the first phase

$$\alpha = \frac{N_1}{N_1 + N_2}. \tag{2.9}$$

For the progress variable α we use a linearized relaxation law

$$\dot{\alpha} = \frac{1}{\tau_\mu}(\alpha - \alpha_{eq}), \tag{2.10}$$

where τ_μ is the relaxation time of the chemical equilibration. The value α_{eq} corresponds to free energy minimum; the phase transition is driven by the deviation from equilibrium.

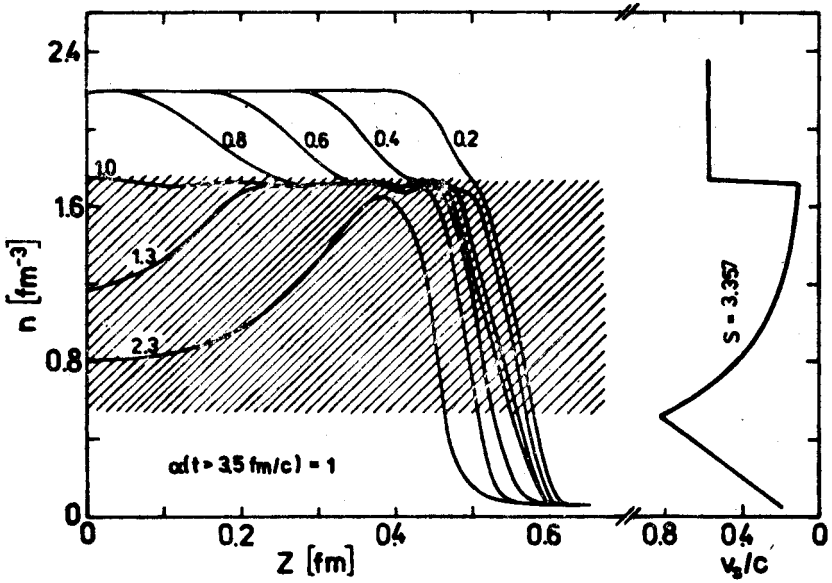

Fig. 2a

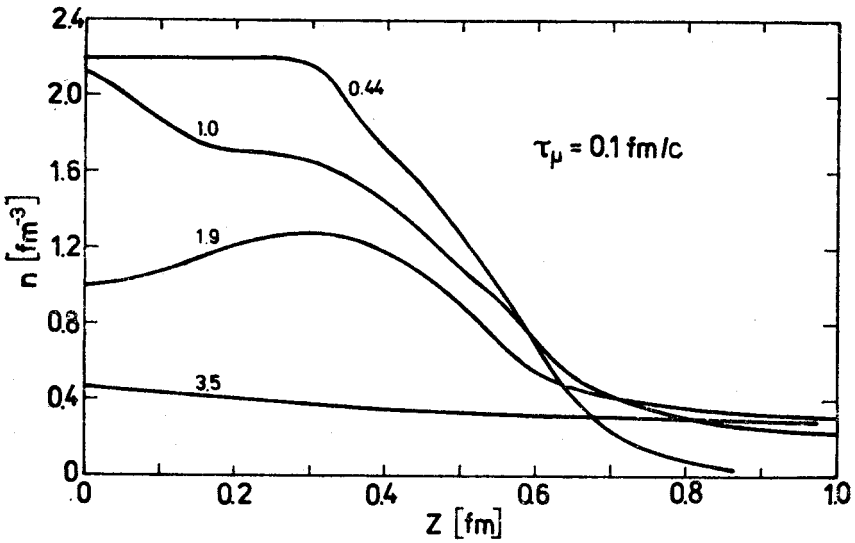

Fig. 2b

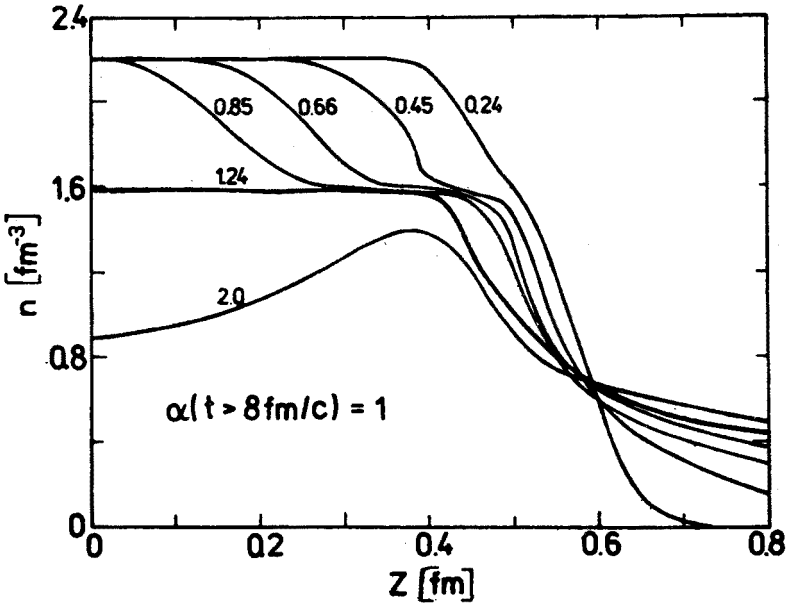

Fig. 2c

Fig. 2. Snapshots of density profiles during plane-symmetric expansion; initial conditions as for Fig. 1a. a) Isentropic expansion (the hatched area indicates the coexistence region); sound velocity on the given isentrope, b) delayed phase transition is included; $\tau_\mu = 0.1$ fm/c, c) gas viscosity is included

Reasonable values of τ_μ are expected to be in the order of the QCD time scale $\hbar/B^{1/4} \sim 1$ fm/c.

The evolution depends on the value of τ_μ. For spherical symmetry $\tau_\mu = 0.1$ fm/c leads again to a shrinking plasma blob as in Fig. 1a; if $\tau_\mu > 0.5$ fm/c the separating front is smeared out. Fig. 2b displays a plane-symmetric expansion with the same initial conditions as in Fig. 2a and with $\tau_\mu = 0.1$ fm/c. One can conclude that the sharp front disappears even at relatively short relaxation times. The reason of this change of the flow pattern is simply the change of the sound velocity; as shown in Ref. [14], the relevant quantity is the frozen local sound velocity c_{fr}

$$c_{\mathrm{fr}}^2 = \frac{\partial p(e, s; \alpha)}{\partial e} > c^2(\tau = 0) \tag{2.11}$$

which is discontinuous at $\tau \to 0$.

In a non-equilibrium phase transition some entropy is produced as it was shown in Refs [11–13]. For the comoving time derivative of the specific entropy s one obtains

$$\dot{s} = \dot{\alpha}(\mu_2 - \mu_1)/T. \tag{2.12}$$

Fig. 3 shows the total extra entropy in the plane-symmetric model at $\tau_\mu = 1$ fm/c for various initial states reachable by shock compression of ground state nuclear matter. One can see that the extra specific entropy is ca. between 1 and 2. Obviously a substantial de-

pendence is expected on τ_μ; the calculations show that ΔS is maximal at $\tau_\mu \simeq 1$ fm/c (cf. Fig. 4), while the transition is not completed until break up if $\tau_\mu > 5$ fm/c. This may be a consequence of the fact that then the relaxation time is comparable to the time of the expansion, however, so far from equilibrium the linear Ansatz (2.10) is rather a rough approximation. For completeness' sake we calculated the entropy increase for the "softer" initial conditions ($3 < n/n_0 < 5$, $T = 200$ MeV) too, but there the increase is rather small, between 2 and 5%.

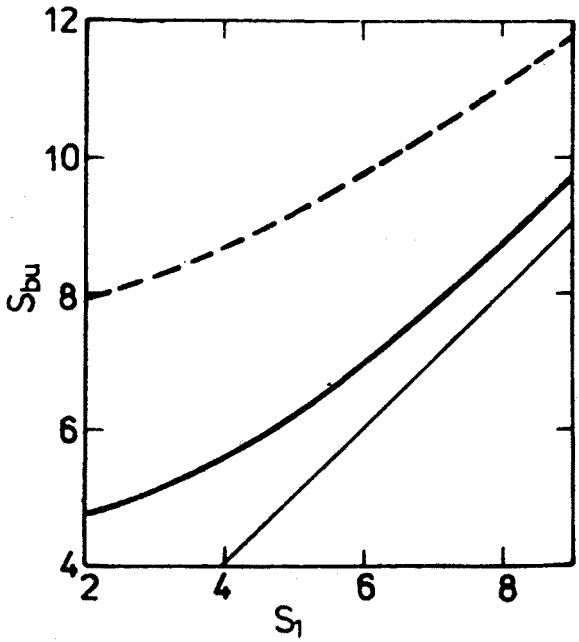

Fig. 3. Final state entropy versus initial entropy for $\tau_\mu = 1$ fm/c. Initial states are plasma states reached from ground state nuclear matter by shock compression; the expansion is plane-symmetric. Dashed line: outermost cells, full line: central part

Case c) *Viscosity effects*

In a realistic situation the delayed phase transition is only one of the sources of entropy production; there are irreversible processes even within one phase. Most familiar representative of such irreversible processes is the viscosity. In a plane-symmetric flow both the shear and the bulk viscosity enter the equations of motion as corrections to the pressure

$$p_{\text{vis}} = p - (\xi + 4\eta/3) u^r{}_{;r}. \tag{2.13}$$

The entropy production of viscous processes is

$$\dot{s} = \frac{1}{Tn} (\xi + \tfrac{4}{3}\eta) \left(\frac{\dot{n}}{n}\right)^2. \tag{2.14}$$

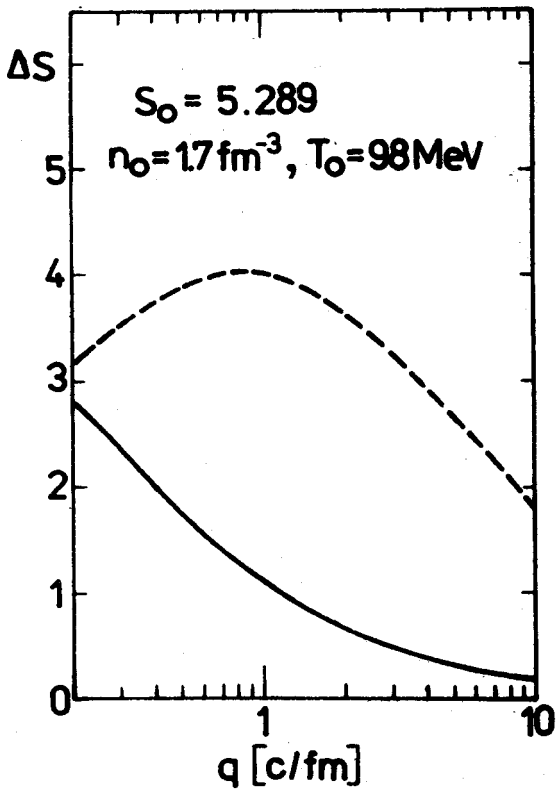

Fig. 4. Entropy production due to delayed phase transition versus the inverse relaxation time $q = 1/\tau_\mu$; plane-symmetric expansion. Dashed line: outermost cells, full line: central part. For $q < 0.2\ c/\text{fm}$ the phase transition is not completed until break-up

Ref. [7] investigated such a non-equilibrium phase transition as a possible source of the bulk viscosity. Since in this paper relaxation phenomena are explicitly incorporated, we can concentrate on the shear viscosity. Viscosity estimates can be found in Refs [7] and [15] for nuclear matter and for plasma. However, in the coexistence region the problem is more complicated; the two viscosity coefficients can be volume averaged only if the droplets of the individual phases are large enough, otherwise the results of the kinetic theory for mixtures suggest a different formula [16]. So, $\eta(n, T)$ is model-dependent in the coexistence region; for illustrative purposes here we simply use the common gas viscosity as in Ref. [12]. Fig. 2c displays the snapshots of density profiles for the same initial conditions as in Fig. 2a. A reheating can be observed due to conversion of kinetic energy into excitation; in the particular case the increase of the specific entropy is ca. 1. The absolute maximum of the entropy increase could be expected in an isoergic expansion (where the internal energy remains constant, since nothing is converted into flow). As an example one can consider a blob initially at $n = 1\ \text{fm}^{-3}$ and $T = 180$ MeV. After isoergic rehadronisation $s = 25$, which is rather unrealisticaly large.

3. *Bubbles and fronts*

Now we are going to turn to investigating discontinuities separating the quark-gluon plasma from nuclear matter. Such discontinuities represent the (planar) idealisation of various fronts as surface regions of growing hadronic bubbles, condensation fronts surrounding plasma blobs or time-like fronts in rapid transitions. Possible initial states for the plasma and final states for the hadronic matter are to be discussed here.

Let us consider a discontinuity with either space-like or time-like normal vector Λ^i. In the following discussions Λ^i is normalized to a unit vector. By integrating the balance equations through the discontinuity one obtains [17, 18]

$$[T^{ir}]\Lambda_r = 0, \tag{3.1}$$

$$[nu^r]\Lambda_r = 0, \tag{3.2}$$

where the bracket denotes the jump. Eq. (3.1) always holds, while Eq. (3.2) is a consequence of particle conservation, so it is valid only for conserved components. The gradients of the thermodynamic intensives are expected to be maximal in the region represented here by the discontinuity, therefore one may assume that transfer processes are moderate outside, and a perfect fluid approximation

$$T^{ik} = (e+p)u^iu^k + pg^{ik} \tag{3.3}$$

can be used there (g^{ik} is of course a Minkowski metric tensor, being the gravity irrelevant, the signature is $+2$). Calculating the three-velocities from Eqs (3.1) and (3.3) before and behind the front one obtains

$$v_1 = \left(\frac{(e_2-e_1)(p_2+e_1)}{(p_2-p_1)(p_1+e_2)}\right)^{-\frac{1}{2}\Lambda^2},$$

$$v_2 = \left(\frac{(e_2-e_1)(p_1+e_2)}{(p_2-p_1)(p_2+e_1)}\right)^{-\frac{1}{2}\Lambda^2}. \tag{3.4}$$

If there is a conserved particle number n, the velocities can be eliminated, and one gets a relation between thermodynamic quantities

$$x_1^2n_1^2 - x_2^2n_2^2 + (p_2-p_1)(x_1+x_2) = 0,$$

$$x = (e+p)n^{-2}, \tag{3.5}$$

where x is called generalised specific volume, and Eq. (3.5) is known as Rankine-Hugoniot-Taub equation. The current through the discontinuity satisfies the relation

$$-j^2 = \Lambda^2 \frac{p_1-p_2}{x_2-x_1} > 0. \tag{3.6}$$

The Second Law prescribes that the entropy current does not decrease while crossing the discontinuity, i.e.

$$[snu^i]\Lambda_i \geqslant 0. \tag{3.7}$$

For $\Lambda^2 = +1$ the discontinuity is a front in the three-space, separating two subvolumes of the matter, e.g. a shock, deflagration, detonation or condensation front. The case $\Lambda^2 = -1$ describes an instantaneous (or rapid) change of the whole volume from one state to another. The incorporation of this latter possibility extends the original Rankine-Hugoniot-Taub analysis to temporal evolution, so relating the section $(p_1-p_2)/(x_2-x_1) < 0$ of the adiabat to physical processes [19]. Now we are going to discuss different particular kinds of fronts. Observe that for $\Lambda^2 = +1$ the positivity of the entropy production (3.7), together with relation (3.6) and the existence of real three velocities (3.4) leads to the inequalities

$$s_2 \geqslant s_1,$$

$$\frac{p_2-p_1}{e_2-e_1} > 0,$$

$$\frac{p_2-p_1}{x_1-x_2} > 0, \tag{3.8}$$

and then there are three different possible types of transmutations as follows:

1) slow (rarefaction) deflagration: $n_2 < n_1,\ p_2 < p_1,\ v_2 > v_1,\ v_{1,2} < c_{1,2}$;

2) fast (compression) deflagration: $n_2 > n_1,\ p_2 > p_1,\ v_2 < v_1,\ v_{1,2} > c_{1,2}$; and

3) fast (compression) detonation: $n_2 > n_1, p_2 > p_1, v_2 < v_1, v_1 > c_1, v_2 < c_2$, (3.9)

where c_i stands for the sound velocity in the particular state.

The nuclear equation of state is not a simple relation $e = e(p)$ as for the bag model equation of state for the plasma, therefore generally the solutions of the Rankine-Hugoniot-Taub equation are to be calculated numerically.

Case a) *Deflagration*

Let us consider first a slow deflagration. Then conditions (3.9) prescribe $p_1 > 0$, being the pressure nonnegative for nuclear matter at or above normal nuclear density. Fig. 5 shows the permitted plasma initial states on the phase diagram. A particular adigaat is depicted in the inset. The deflagration adiabats are convex curves on the (p, x) diagram, bound by a Chapman-Jouguet point where the entropy reaches a maximum. The possible final states represent hot and moderately dense nuclear matter between 50 and 150 MeV temperatures and below 0.5 fm^{-3} density. One can observe that for $5 < s_1 < 22$ the initial state is in the coexistence region, so the slow deflagration can start only from a supercooled plasma, which needs a delayed phase transition.

For definiteness' sake here we consider the deflagration to final states corresponding to the Chapman-Jouguet point. Figs 6 and 7 display some final state variables. We select initial states on the phase boundary (cf. Fig. 6) and on the dashed line of Fig. 5, defined by the equations

$$n = n(T, \mu = 1.1\mu_0), \tag{3.10}$$

$$p(T, \mu_0) = 0,$$

(cf. Fig. 7). The rather large entropy increase for the deflagrating low entropy plasma has already been mentioned by Stöcker [10].

In a deflagrating plasma blob at rest the front proceeds with the velocity $v_{\mathrm{def}} = v_1$ (cf. Eq. (3.4)), while the hadronic matter is ejected with

$$v_{\mathrm{out}} = \frac{v_1 - v_2}{1 - v_1 v_2} \equiv v_{12}. \tag{3.11}$$

The front velocity is now considerably greater than that for vanishing baryon density (compare Figs 6 and 7 with Fig. 8 in Ref. [6]). In the previous Section we mentioned that in a spherical expansion of a very baryon-rich state the velocity of the transition region between hadrons and plasma is found to be of the order of 0.1 c. Comparing this value to Figs 6 and 7 one can conclude that the slow deflagration is a serious candidate for the rehadronization process of a cool plasma.

Let us consider now deflagration bubbles with hadronic matter inside and plasma outside (cf. Ref. [6] for introducing this idea). Then the growth velocity of the hadronic bubble is $v_{\mathrm{gr}} = v_2$. In a medium of finite baryon charge the slow deflagration is bounded by $v_2 \leqslant c_2$, equality holds at the Chapman-Jouguet point. For $v_2 > c_2$ the front is absolutely unstable [20]. Consequently, in contrast to the case $\mu = 0$ [6], at large baryon densities we find v_{gr} in the same order of magnitudes as v_{def} (cf. Figs. 6 and 7).

A growing hadronic bubble (with matter at rest inside) surrounded by a non-flowing

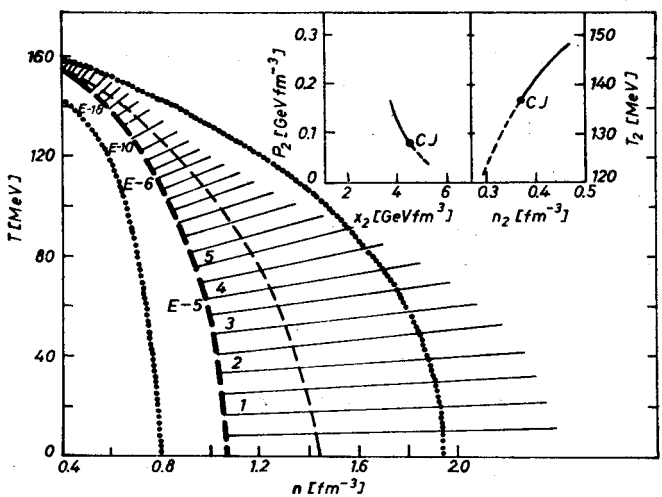

Fig. 5. Permitted region of plasma states whence slow deflagration is possible into hadronic matter; temperature versus density plot. The hatched area with lines indicates the permitted region, the lines are isentropes. The phase equilibrium boundaries are displayed by dotted lines. The heavy dashed line indicates states with 0 plasma pressure; it almost coincides with the spinodal boundary. The dashed line in the metastable region shows the initial states discussed in the text. The numbers left from the line $p_{\mathrm{q}} = 0$ indicate nucleation rates in c/fm^4 (logarithmic notation). The inset displays a deflagration adiabat (full line: physical section) belonging to an initial state on the $s = 5$ isentrope indicated by a cross. CJ is the Chapman-Jouguet point below which the deflagration front is unstable (dashed line)

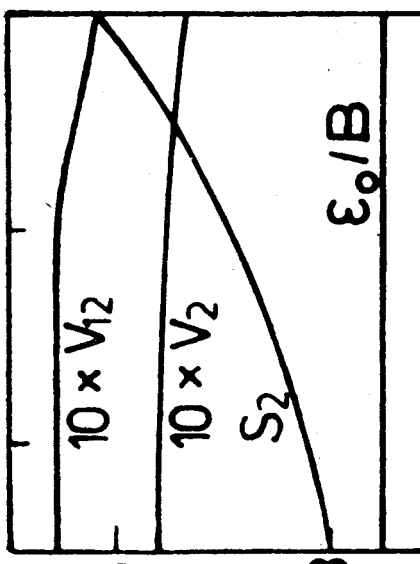

Fig. 6

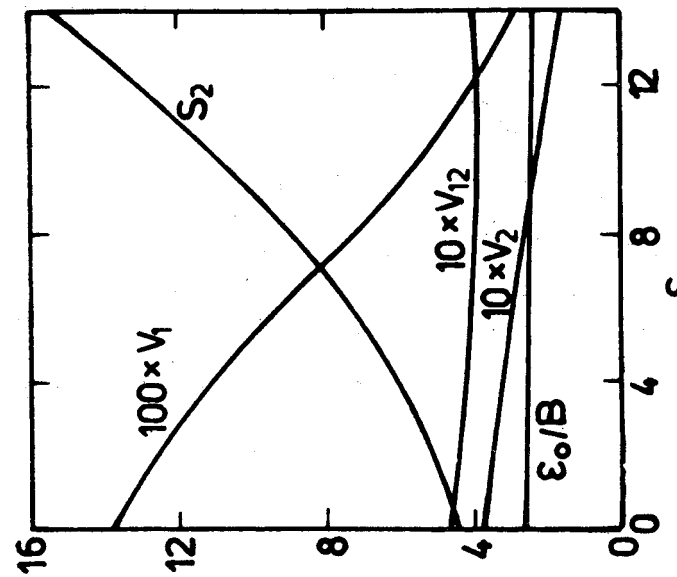

Fig. 7

Fig. 6. Some final state variables for deflagration from the phase boundary to the Chapman-Jouguet point (details in the text)

Fig. 7. As Fig. 6, but with initial states on the light dashed line of Fig. 5

plasma must drive a shock wave into the plasma in order to fulfil the boundary conditions. Then there is a relation amongst the energy density of the far region of the plasma at rest e_0, that of flowing outward from the bubble e_1 and the velocity difference across the rehadronisation front v_{12}:

$$v_{12}^2 = \frac{3(e_1 - e_0)^2}{(3e_0 + e_1 - 4B)(3e_1 + e_0 - 4B)}. \tag{3.12}$$

The plasma energy density e_0 is displayed in Figs 6 and 7.

In the adopted situation a strong supercooling is needed in the initial plasma state so that $p_0 < 0$. Nevertheless, the discussed particular final states correspond to the Chapman-Jouguet point as was mentioned above. In other cases initial states of $p_0 > 0$ are quite allowed. However, then the bubble growth velocity v_{gr} becomes small and the dominating hadronization process is bubble creation rather than bubble growing. Note that phase space considerations do not fix all the parameters of the growth; one of them

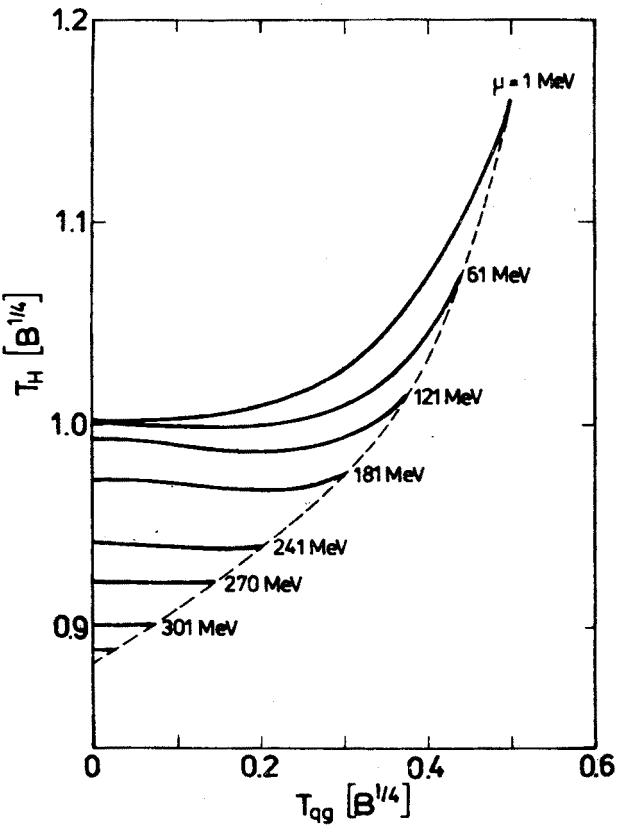

Fig. 8. Hadronic temperatures versus plasma temperatures for bulk transition. Plasma initial states are parametrized by the chemical potential. Entropy production would be negative on the right hand side of the dashed line

remains free and should be calculated in a complete picture including diffusion processes, heat flow between the phases and the interface kinetics. This task is far from being consistently solvable (even with static boundary conditions) since the relevant material constants are poorly known. In the present exploratory study we have analysed only the hydrodynamic component of this complex problem.

For a fast deflagration the necessary conditions are very similar to those in a detonation (cf. conditions (3.9)), the only difference is that the flow is not subsonic in the second phase. Therefore we do not discuss this particular subcase here.

We can list the conclusions of this subsection as follows:

1) the deflagration front is a candidate for the rehadronisation process of a cool plasma; and

2) slowly growing deflagration bubbles are possible candidates for homogeneous nucleation; their initial conditions are not exotic (i.e. mechanically unstable [21–23]) with negative pressure.

The preshock waves emitted by the deflagration bubbles cause, when meeting, irregular (turbulent) flow in the medium. (The arising fluctuations then may act as impurities, causing, in the late transition stage, a heterogeneous nucleation.) The resulting characteristic rapidity fluctuations have been mentioned by Gyulassy et al. [6] as signals of the nucleation process.

Case b) *Detonation*

Constructing the detonation solutions (see conditions (3.9)) of Eq. (3.5) with the equations of state (2.3–5) we find that the corresponding initial plasma states are characterized by $p < 0$ and $n_1 < 0.4\,\mathrm{fm}^{-3}$, while for the final hadronic states $T_2 > 500$ MeV. Both states seem to be exotic. Let us discuss separately the initial and final states.

At $p < 0$ the matter is unstable against a decay into a non-homogeneous state (cf. e.g., droplets) [21–23]. However, such states can be quite reasonable from thermodynamic viewpoint [21, 24] and the droplet formation needs some time. Therefore states with $p < 0$ can be reached. As it was shown in a different context [25] the inertial forces can drive the expanding system farther till the negative pressure becomes operative, stopping and reversing the expansion and causing a fisseling (fragmentation). Dynamical calculations with suppressed phase transition ($\tau_\mu \to \infty$) show that the initial configurations considered in Sect. 2 reach the minimum energy density outside the region, where detonation can formally happen.

One has to notice that the droplet picture breaks down at large supercooling. The Cahn-Hilliard theory [26] claims that the distinction between a limited surface region and a homogeneous interior of droplets fails even at moderate supercooling. At strong supercooling the development of the new phase proceeds via spinodal decomposition; near the spinodals the potential barrier vanishes and very small fluctuations of large spatial extension trigger the development of the new phase. Before reaching the spinodal the phase separation happens faster via thermal fluctuations of activation energy $\sim T$. For such fluctuations the size remains finite and the correlation length, which is more or less the surface thickness, is in the order of the droplet radius. Therefore the picture of droplets with sharp surface fails in the spinodal region. For a detailed discussion see Ref. [27].

In the two-phase model under consideration the matter is per definitionem stable, no turning point of the Helmholtz free energy $f(n, T)$ or loop in $p(\mu, T)$ [28] exists. However, in terms of the Cahn-Hilliard theory the potential barrier vanishes at $f_q = f_n + f_\pi$. This defines the boundary of metastability (cf. Fig. 5). It is remarkable that the spinodal almost coincides with the line $p_q = 0$; the unstable region, familiar from van der Waals type liquid-gas transitions is degenerated to a line. In a more complete model based on equal footing on both phases $f(n, T)$ will be a smooth function with turning points $f_{nn} = 0$ and with a finite unstable region. So we consider our spinodal construction as an optimistic limit for the metastable region beyond which the homogeneous initial phase can no longer exist.

For the final states, we can note that according to present general opinion $T = 500$ MeV is far above the deconfinement temperature (generally estimated as 150–200 MeV). The existence of a so superheated hadronic matter seems to be improbable.

Therefore we can conclude that, although detonation bubbles offer interesting consequence [6], fast deflagration and detonation bubble growth cannot be expected in baryon-rich situations. For $\mu = 0$ the above considerations are not necessarily valid in their present form.

Case c) *Bulk transition*

Now we turn to $\Lambda^2 = -1$, when the hypersurface is time-like. Since then the two states are separated in time, this is an instantaneous (or rapid) transition in a whole volume. Such a picture can be applied to the vanishing central part of a decaying plasma blob, or to the coalescence stage when the last islands of the plasma are vanishing, or to the spontaneous appearance of the hadronic bubbles.

Because of symmetry considerations $v_1 = v_2 = 0$ must hold. But then Eq. (3.4) leads to $e_1 = e_2$, and j^2 in Eq. (3.6) becomes simply $-n^2$. Hence $n_1 = n_2$, and thus Eq. (3.5) reduces to an identity. In Fig. 8 the possible final hadronic temperatures versus initial plasma temperatures are displayed. Our Figure deals with the generic case; the special case $\mu = 0$ has been investigated in Ref. [4]. Let us observe that, due to the entropy condition (3.8), the possible initial and final states are concentrated on rather small regions. The final hadronic temperatures seem to be slightly above the deconfinement temperature while the initial plasma states possess negative pressures; both states are beyond the spinodals. Again, the physical relevance of such a rehadronization picture is questionable.

The considered bulk transition corresponds to fluctuations at constant density, while in classical nucleation theory the density or particle number fluctuations dominate in creating the critical bubbles. The latter processes are related to flow or diffusion of baryon number, and, therefore, do not belong to our model.

In all the processes discussed in this Section considerations about the microscopically determined rate of the hadronic phase creation were important. Therefore we close this Section by some order of magnitude estimates relying on classical nucleation theory. In accordance with Ref. [29] the nucleation rate via thermal fluctuactions is

$$w = w_0 T_c^4 \exp\left(-\frac{16\pi\alpha^3}{3T(p_1 - p_2)^2}\right), \tag{3.13}$$

where T_c is the critical temperature (cf. Eq. (2.7)), while α stands for the surface tension

$$\alpha = \alpha_0 T_c^{1/3} p_c^{2/3}. \tag{3.14}$$

Here p_c is the pressure of the critical state, while the two still undefined factors w_0 and α_0 are dimensionless smooth functions expected in the order of 1. Critical bubble radii are given by

$$R_{cr} = \frac{2\alpha}{p_1 - p_2}. \tag{3.15}$$

The pressures of both phases are to be calculated at the same temperature and chemical potential, thus giving equilibrium bubbles [29].

Note that here quantum fluctuations are ignored. They become important below the equivalent quantum temperature T_{eq}, estimated as

$$T_{eq} \sim \frac{8 \text{ Mev}^{1/2} \text{ fm}}{|n_1 - n_2|} \sqrt{\frac{\alpha n_1}{R_{cr}^3}}. \tag{3.16}$$

Typical values are of the order of 10 MeV, which is well below the temperatures considered in this paper.

The radius of critical bubbles is smaller than 10 fm if the supercooling is about 10 MeV, for stronger supercooling it rapidly approaches values between 1 and 3 fm. Since the expected extension of the deconfined state is moderate, a few such bubbles will complete the confinement transition.

The rate (3.13) is exceedingly small in the metastable region; some representative numbers are indicated on the $p_q = 0$ line of Fig. 5. For $s_q > 3$ the maximum values of w lie deeply inside the region $p_q < 0$.

The increase of the volume V_2 of the new phase proceeds via both bubble creation and bubble growth. Thus

$$\dot{V}_2(t) = \frac{4\pi}{3}(V(t) - V_2(t)) w R_{cr}^3$$

$$+ 4\pi \int_{t_c}^{t} w(t')\,(V(t') - V_2(t')) v_{gr}(t')\,[R_{cr}(t') + \int_{t'}^{t} v_{gr}(t'')dt'']^2 dt'. \tag{3.17}$$

It is convenient to use the volume fraction $x_2 = V_2/V$. Now, Eq. (3.17) is rather complicated for practical use. In tackling early cosmology usually the Avrami approximation is exploited, which results for isothermal nucleation in

$$x_2(t) = 1 - \exp\{-[(t - t_c)/\tilde{t}_0]^4\},$$

$$\tilde{t}_0 = (\pi w v_{gr}^3/3)^{-1/4}, \tag{3.18}$$

where t_c denotes the time moment when $T = T_c$. Another possibility is to turn to the Ruckenstein-Ihm approximation; then Eq. (3.17) reduces to

$$\dot{x}_2(t) = 4\pi v_{gr}(t) \int_{t_c}^{t} w(t')\,(1-x_2(t')) \int_{t'}^{t} [v_{gr}(t'')dt'']^2 dt'. \tag{3.19}$$

This equation can be converted into an integral equation of Volterra type II; for isothermal case the solution is

$$x_2(t) = 1-\sqrt{2}\sin\left[(t-t_c)/t_0+4/\pi\right]\exp\left\{-(t-t_c)/t_0\right\},$$

$$t_0 = (2\pi w v_{gr}^3)^{-1/4}. \tag{3.20}$$

While the forms of the expressions $x_2(t)$ in Eqs. (3.18) and (3.20) are not the same, the characteristic times differ only in a factor $6^{1/4}$, which is rather irrelevant w_0 being unknown. Therefore choice between approximations will not be further discussed here; we use Eq. (3.20) for estimation.

At $t = t_c+2t_0$, $x_2 = 0.95$. Thus $2t_0$ can be regarded as the time needed for transformation into hadrons.

Now, for a simple estimation one can choose the rate values in Fig. 5 between 10^{-6} and 10^{-18} c/fm^4, $v_{gr}/c \sim 0.1$ and $w_0 = \alpha_0 = 1$. Then the necessary time scale is rather long, 10^2 fm/$c < t_0 < 10^5$ fm/c. These results, even as estimates, involve strong simplifications (as the crude pre-equilibrium factors in Eqs (3.13–14); neglect of both the time lag of the fluctuation development and the vanishing barrier at the spinodal), nevertheless they give some hint for a noticeable supercooling and strong non-equilibrium phenomena during the rehadronisation. If the nucleation time scales are indeed so long compared to those of the hydrodynamical expansion, then the spinodal decomposition seems to be the relevant decay process; it may be enhanced by mechanical instabilities at negative pressures.

4. Hadron yields

Until now we investigated the hydrodynamical regime of evolution. Nevertheless, the observables are particle numbers and distributions, detected after break-up. The connection between the data of the hydrodynamic calculation and these observables is not trivial from at least three reasons. First, our hadronic equation of state contains only two components, nucleons and massless pions. Second, even if it were to contain various particle components, the detected particle numbers and distributions might differ from those in the hydrodynamic description, as shown in an explicit example in Ref. [30]. Third, different compositions may lead to the same dynamic behaviour, as discussed in Ref. [31]. These considerations suggest that a complete model should contain not only the description of the hydrodynamic evolution but clear break-up prescriptions as well.

Of course the break-up happens in the hadronic phase, after some hadrochemical processes. Nevertheless, in simplified models the phase transition and the break-up may be contracted to the same moment. This will be done here too.

The redistribution of quarks into hadrons is obviously a complex process. One may expect that the final yields depend on three kinds of data: characteristics of the initial plasma state, those of the final hadronic state and the history of the phase transition. Concealing the third one by some averaging and discussing only the dependence on the first two, one can clearly distinguish extreme models.

The first is when hadron yields depend only on final state data. This means chemical equilibrium, but, at least for strange particle production, it is ruled out by observations, the predicted K yields being extremely high [32]. It is better to choose the other possibility, when the yields depend only on initial state characteristics: this is the combinatoric model, when hadron numbers are proportional to the corresponding quark-quark collisions [33]. It predicts reasonably low kaon numbers at moderate energies.

Now we propose a modified model interpolating between extremal possibilities. First let us recapitulate some elements of the combinatoric model. It assumes that the unnormalized probability of a particular hadron production is proportional to all the number of quark constituents (collision probability) and also of a channel factor (distinguishing between e.g. meson and baryon formation). The quark numbers are given, and the channel factors can be determined from balance equations expressing, for example, the assumption that there is no annihilation. Then there are four such equations:

$$Q = \mathrm{K}+\pi+2\mathrm{Y}+\Xi+3N,$$

$$S = \bar{\mathrm{K}}+\eta+\mathrm{Y}+2\Xi+3\Omega, \tag{4.1}$$

$$+ \text{ conjugate equations for antiparticles,}$$

where letters stand for particle numbers of the indicated particles, and Y is a common name for Λ and Σ. These four equations can be satisfied by four channel factors in the generic case (here we choose a distinction between formation of mesons containing and not containing S quarks, and the same for baryons); because of symmetries in the original combinatoric model the number of different channel factors reduces to 2 [33].

Now, one can assume that the probability of the appearance of a particular hadron as final state is proportional both to the initial probability (given by e.g. the combinatoric model) and to the number of microstates belonging to the particular hadronic final state. These statistical weight factors f_i can be calculated from thermodynamics.

The statistic definition of the entropy shows that the number of microstates is measured by e^S. Nevertheless, when using temperature instead of energy as a fundamental variable, the proper potential is [34]

$$S - \frac{1}{T} E = -\frac{1}{T} F, \tag{4.2}$$

where F is the free energy. So one would expect $e^{-F/T}$ as a statistical weight, as it is, in fact, used in e.g. Ref. [35] (cf. also footnote 8 of Ref. [36]). Nevertheless, F belongs to the whole continuum of all the components, in the present context we are rather interested in the changes of F for unit changes of the particle numbers, which are the chemical potentials.

So one would expect

$$f_i \sim e^{-\tilde{\mu}_i/\tilde{T}}, \tag{4.3}$$

where the tilde indicates final state variables.

Now, this model is straightforward if $\tilde{\mu}_i$ and $\tilde{T}$ are known, since the four channel factors can be calculated from the balance equations (4.1), collision probabilities are determined by the quark numbers, and the factors f_i are given by Eq. (4.3). Nevertheless, in order to obtain $\tilde{\mu}_i$ and $\tilde{T}$ one should either follow the dynamics of the phase transition, or perform some self-consistency calculations. (Note, e.g. that, according to observations, there is definitely no chemical equilibrium in the final state [32].) Here we want to give only estimations, so the problems will be avoided by two simplifying assumptions. First, the leading term in Eq. (4.3) will be used:

$$f_i \sim e^{-m_i/\tilde{T}}, \tag{4.4}$$

where m_i stand for particle masses; this approximation has become independent of assumptions for chemical equilibrium. Second, we consider an isothermal phase transition, when

$$\tilde{T} = T \tag{4.5}$$

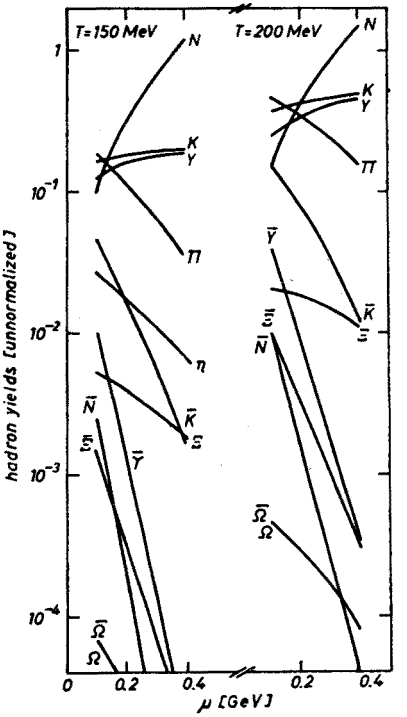

Fig. 9. Unnormalized hadron yields versus plasma chemical potential at freeze-out, for two different hadronic temperatures

and choose some reasonable freeze-out temperature. Then the yields depend on the plasma intensities T and μ; in Fig. 9 we display the dependence on μ for two characteristic temperatures.

One can observe the nucleon dominance for $\mu > 200$ MeV; surprisingly kaons and lambdas are more frequent than pions. The rare hadrons are now suppressed due to their large masses, for the dominant components the relative yield; are similar to the predictions of Ref. [33]. Our predictions for the ratios $\overline{Y}/Y$ and $\overline{K}/K$ are in the same order of the magnitude as in the nuclear fireball model [37], thus these ratios are not useful as plasma signals.

Comparing our model to the combinatoric one, a possible conclusion is that the two different models confirm each other for K and Λ yields; the rare hadron yields depend on the details of the models, and more definite statements should be also preceded by developing a consequent method for calculating $\tilde{T}$.

One may also discuss another freeze-out possibilities e.g. such that the rehadronization is so fast that the energy density is constant during it. Taking the thermal equilibrium distributions for individual hadron species the picture resembles the detonation scenario. Nevertheless we have seen that the detonation picture leads to too high superheating, so it does not seem to be physical.

There is always the concurrent possibility that the plasma has not been formed. Therefore the yields predicted by plasma rehadronisation and by hadrochemistry [38] are to be compared at the investigated energies in order to get plasma signals.

5. Discussion and summary

In this paper we have investigated the rehadronization of a baryon-rich plasma on different levels. First the hydrodynamical expansion of quark-gluon plasma blobs was studied with some idealisations as Maxwell's construction or, alternatively, a linear relaxation model for phase transitions, spherical or planar symmetry in the expansion and the use of a gas viscosity. It is found that the expansion pattern essentially depends on the viscosity and on the delay in the phase transition. If both effects are negligible, then the expansion of the cold plasma can be described as a shrinking droplet evaporating hadrons from its surface (it can be considered as a condensation front, being the source of considerable entropy production). Initially hotter plasma blobs expand without any clear front; the entropy increase is on the 10% level.

The transition in idealized fronts was also analysed. We found slowly deflagrating bubbles, and estimated $v_{gr}/c \sim 0.1$ for the bubble growth velocity. Unique value cannot be obtained without incorporating diffusion, heat conduction and interface kinetics. The entropy production of initially hot plasmas is moderate ($\sim 10\%$) so then entropy provides a window into early hot stages. Bubble growth in cold plasmas tends to close this window due to substantial entropy increase.

The analysis of detonation bubbles and bulk transitions was made here first time for a medium of finite baryon charge. The plasma initial states are required to be strongly supercooled (far inside the mechanically unstable region $p < 0$), and the final hadronic

states are overheated (strongly for detonation and moderately for bulk transition). Whether such transformations are liable or not, it should be decided by further work based on dynamical calculations on the compression stage, proper treatment of curvature, surface and final size effects.

Some estimates of nucleation rates according to the classical droplet model are presented. While these estimates are not on safe ground, a comparison with hydrodynamic time scales gives some hints for substantial supercooling and strongly nonequilibrium character of the phase transition.

The combinatoric rehadronisation model is more related to observable plasma signals. We have introduced statistical weights for different hadrons corresponding to the numbers of possible final states. Assuming thermal equilibrium between the plasma and the hadrons definite predictions have been obtained for the relative yields. The high kaon and lambda yields conform to the results of previous investigations; for other particles (except, of course, protons and pions) the predictions seem to depend on the details of the models. If the emerging hadrons remain in contact with each other for sufficiently long time, they develop towards chemical equilibrium. In any case, the yields suggest that kaons and lambdas should be incorporated into the hadronic equation of state.

In conclusion: we considered the decay of the baryon-rich plasma in three issues: a) hydrodynamic expansion; b) space-like or time-like fronts (discontinuities) between the quark plasma and hadronic matter; and c) the emerging hadron yields. These items can serve as bases for further detailed investigations.

Authors would like to thank Dr. J. Zimányi for illuminating discussions.

REFERENCES

[1] M. Jacob, H. Satz (eds.), Proc. Workshop on Quark Matter Formation and Heavy Ion Collisions, World Scientific, Singapore 1982.

[2] R. Anishetty, P. Koehler, L. McLerran, *Phys. Rev.* **D22**, 2793 (1980); J. D. Bjorken, *Phys. Rev.* **D27**, 140 (1983); K. Kajantie, L. McLerran, *Nucl. Phys.* **B214**, 261 (1983).

[3] B. Banerjee, N. K. Glendenning, T. Matsui, *Phys. Lett.* **127B**, 453 (1983).

[4] N. K. Glendenning, T. Matsui, *Phys. Lett.* **141B**, 419 (1984).

[5] G. Baym, B. L. Friman, J. P. Blaizot, M. Soyer, W. Czyż, *Nucl. Phys.* **A407**, 541 (1983); B. L. Friman, G. Baym, J. P. Blaizot, *Phys. Lett.* **132B**, 291 (1983).

[6] M. Gyulassy, K. Kajantie, H. Kurki-Suomio, L. McLerran, *Nucl. Phys.* **B237**, 477 (1984).

[7] M. Gyulassy, T. Matsui, *Phys. Rev.* **D29**, 419 (1984); P. Danielewicz, M. Gyulassy, LBL-17287.

[8] K. Kajantie, L. McLerran, *Nucl. Phys.* **B222**, 152 (1983).

[9] M. Gyulassy, in Proc. 6th Int. Bálaton Conf. on Nucl. Phys. ed. J. Erö, 1983.

[10] H. Stöcker, *Nucl. Phys.* **A418**, 587 (1984).

[11] B. Kämpfer, B. Lukàcs, KFKI-1984-100.

[12] H. W. Barz, B. Kämpfer, L. P. Csernai, B. Lukàcs, *Phys. Lett.* **143B**, 334 (1984); L. P. Csernai, H. W. Barz, B. Kämpfer, B. Lukàcs, *Phys. Rev.* **C31**, 268 (1985).

[13] L. P. Csernai, B. Lukàcs, *Phys. Lett.* **132B**, 295 (1983).

[14] L. J. F. Boer, *Appl. Sci. Res.* **A2**, 447 (1951).

[15] P. Danielewicz, *Phys. Lett.* **146B**, 168 (1984); S. Gavin, *Nucl. Phys.* **A435**, 826 (1985).

[16] J. O. Hirschfelder, C. F. Curtiss, R. B. Bird, *Molecular Theory of Gases and Liquids*, Wiley, New York 1954.

[17] A. H. Taub, in *Relativity Theory and Astrophysics*, Vol. 1, ed. J. Ehlers, Amer. Math. Soc. Providence, R. I. 1967.
[18] B. Lukàcs, KFKI-1978-82.
[19] L. P. Csernai, T. Matsui, UMTNP-109/1984.
[20] L. D. Landau, E. M. Lifschitz, *Hydrodynamics*, Pergamon Press, London 1959.
[21] P. Danielewicz, *Nucl. Phys.* **A314**, 465 (1979).
[22] B. Lukàcs, L. P. Csernai, Proc. EPS Topic. Conf. on Large Ampl. Coll. Nucl. Motion, Keszthely 1979, p. 662.
[23] B. Lukàcs, L. P. Csernai, *Acta Phys. Slovaca* **34**, 161 (1984).
[24] B. Lukàcs, K. Martinás, KFKI-1984-33.
[25] H. Schulz, B. Kämpfer, H. W. Barz, G. Röpke, J. Bondorf, *Phys. Lett.* **147B**, 17 (1984); B. Kämpfer, H. Schulz, B. Lukàcs, *J. Phys. G* **11**, L47 (1985).
[26] J. W. Cahn, J. E. Hilliard, *J. Chem. Phys.* **31**, 688 (1959).
[27] K. Binder, *Lecture Notes in Physics* **132**, 76 (1980).
[28] L. Diósi, Bettina Keszthelyi, B. Lukàcs, G. Paál, *Astron. Nachr.* **306**, 213 (1985).
[29] T. DeGrand, K. Kajantie, *Phys. Lett.* **147B**, 273 (1984); L. D. Landau, E. M. Lifshitz, *Statistical Physics*, Pergamon Press 1980; E. M. Lifschitz, L. P. Pitajefski, *Physical Kinetics*, Akademie-Verlag, Berlin 1983.
[30] H. W. Barz, B. Lukàcs, J. Zimányi, G. Fài, B. Jakobsson, *Z. Phys.* **A302**, 73 (1981).
[31] B. Lukács, K. Martinás, KFKI-1984-110.
[32] F. Asai, H. Sato, M. Sano, *Phys. Lett.* **98B**, 19 (1981).
[33] T. S. Biró, J. Zimányi, *Nucl. Phys.* **A395**, 525 (1983); Proc. 6th Balaton Conf. on Nucl. Phys., ed. J. Erö, Budapest 1983, p. 495.
[34] L. Diósi, G. Forgács, B. Lukács, H. L. Frisch, *Phys. Rev.* **A29**, 3343 (1984).
[35] A. H. Guth, E. J. Weinberg, *Nucl. Phys.* **B212**, 321 (1983).
[36] A. H. Guth, E. J. Weinberg, *Phys. Rev. Lett.* **45**, 1131 (1980).
[37] P. Koch, J. Rafelski, W. Greiner, *Phys. Lett*, **123B**, 151 (1983).
[38] T. S. Biró, B. Lukács, J. Zimányi, H. W. Barz, *Nucl. Phys.* **B386**, 617 (1982); H. J. Möhring, J. Ranft, S. Ritter, TIS-RP/139/PP, 1984.